Guided Waves on Sinusoidally-Modulated Reactance Surfaces

A. A. OLINER† AND A. HESSEL†

Summary—**A rigorous solution is derived for the propagation characteristics and field distributions of waves guided by a plane surface which possesses a surface reactance modulated sinusoidally in the propagation direction. The explicit field amplitudes and the determinantal equation for the propagation wavenumber are expressed in a continued fraction form which is rapidly convergent for all values of modulation. Numerical results are obtained for both surface wave (modal) and leaky wave (nonmodal) solutions. The relevance of these studies to high-gain modulated surface-wave antennas is discussed.**

I. Introduction

THE present study of guided waves on sinusoidally-modulated reactive surfaces was motivated by recent developments in high-gain end-fire antennas of the surface wave type. A customary method for improving the gain of surface-wave antennas has been to design them according to the Hansen-Woodyard condition. For high gains, however, the surface wave becomes necessarily very loosely bound to the guiding surface, and the performance becomes sensitive to irregularities in the structure. A break-through with regard to this difficulty was offered by Simon[1,2] several years ago; he showed that gains as high as those predicted by the Hansen-Woodyard condition for a comparable antenna length, together with a *tightly*-bound surface wave, were possible when the surface wave structure was modulated along its length. Since then, a variety of modulated surface-wave antennas have been designed, but these designs are largely empirical, being a combination of sinusoidal modulations, tapers, steps, and in-between variations. The theoretical understanding of the control of these effects is still limited, and the state of the art is hampered by this lack of knowledge.

Thomas and Zucker[3] have examined the effect of modulating the phase velocity of a surface wave by employing a spectral representation of the modulation. They show that with either a phase or amplitude modulation, a radiated beam can be produced which is tilted at an arbitrary angle with the surface, and may be made end-fire if desired. They did not, however, as they acknowledge, study the surface parameters required to yield the necessary phase or amplitude distribution. A start in this direction was made by Pease,[4] who considered a dielectric slab, the index of refraction of which was modulated very gently in a sinusoidal fashion. The approximations employed in his analysis, however, which were made to correspond to slow variations, are sufficiently severe as to cast doubt on the practicality of his results. The present study, which is a continuation in this direction, is a rigorous treatment of sinusoidal variations in surface reactance.

The surface under study is a plane surface possessing a reactance that varies sinusoidally in the direction of propagation of the guided waves. If the period, or spacing, of the modulation is sufficiently small, the modulation serves to affect quantitatively the propagation wavenumber of the surface wave guided along it, and to introduce one or more stop bands. If this spacing is larger than some critical value, the modulated surface wave will give rise to one or more leaky waves which *radiate away* from the surface at some angle. Because of its relevance to the antenna problem, only the E (or TM) waves guided by the surface are considered here.

A solution to the problem is obtained by viewing the geometry in terms of modes associated with propagation perpendicular to the surface; these modes are discrete in character and are specified by the periodicity of the modulation. The nature of the impedance boundary condition at the surface is such that each of these modes couples only to itself and to the next higher and lower modes, in contrast to most diffracting surfaces which couple all modes to each other. As a result, the problem reduces to the solution of an infinite set of linear equations in which each equation involves only three modes. Explicit expressions for the field amplitudes of each of these modes (which are equivalent to the space harmonics) and the determinantal equation for the propagation wavenumber along the surface are then expressed in a continued fraction form which is rapidly convergent for all values of modulation. In addition, a very simple explicit expression for the propagation wavenumber is deduced by a perturbation procedure that is valid for small modulation values.

The physical mechanism for the leakage of energy away from the surface wave may be regarded in a fashion analogous to that for the leaky wave produced by a slitted rectangular waveguide, for example. In this latter example, the opening offered by the slit permits the radiation to escape. In the surface wave case, the periodic modulation produces an infinity of discrete

† Microwave Res. Inst., Polytechnic Institute of Brooklyn, Brooklyn, N. Y.

[1] J. C. Simon and V. Biggi, "Un nouveau type d'arien et son application à la transmission de télevision à grande distance," *L'Onde Électrique*, no. 332; November, 1954.

[2] J. C. Simon and G. Weill, "Un nouveau type d'antenne à rayonnement longitudinal," *Ann. de Radioélectricité*, vol. VIII; July, 1953.

[3] A. S. Thomas and F. J. Zucker, "Radiation from Modulated Surface Wave Structures—I," 1957 IRE NATIONAL CONVENTION RECORD, Pt. 1, pp. 153–160.

[4] R. L. Pease, "Radiation from modulated surface wave structures—II," 1957 IRE CONVENTION RECORD, Pt. 2, pp. 161–165.

modes of the type referred to above, all of which are below cutoff if the modulation period is sufficiently small. (An equivalent remark would be that all of the space harmonics are slow waves.) If the modulation period is increased, one or more of these modes may become propagating; power is thus radiated away from the surface wave itself via the mechanism of a higher-order mode introduced by the periodicity.

The characteristics of the surface wave and leaky wave solutions are discussed in Section III. Band structure curves are presented for the surface-wave solutions; of interest is the appearance of stop bands and the involved behavior at the band edges. The relative amplitudes of the various space harmonics are also presented. The discussion on the leaky wave solutions includes the variation of attenuation and phase constants with modulation spacing, or alternatively, with the angle of the radiated wave, and the relative amplitudes of the various radiated beams and the surface wave. The relation to the end-fire antenna problem is also touched upon.

II. Formal Solution

Rigorous solutions are obtained below for the propagation characteristics and field distribution of waves guided by a plane surface which possesses a surface reactance sinusoidally modulated in the propagation direction. The reactive plane surface, which is chosen as the yz plane in Fig. 1, exhibits a surface reactance of the form

$$X(z) = X_s\left[1 + M\cos\left(\frac{2\pi}{a}z\right)\right], \tag{1}$$

where X_s is the constant value of surface reactance about which the modulation is made, M and a are the amplitude and period, respectively, of the modulation, and an exp $(j\omega t)$ time dependence is chosen. The modulation amplitude M is restricted to the range $M \leq 1$. The impedance boundary condition at the plane $x=0$ is, therefore,

$$-\boldsymbol{E}_t(0, y, z) = jX(z)\boldsymbol{H}_t(0, y, z) \times \mathbf{x}_0, \tag{2}$$

where $\boldsymbol{E}_t$ and $\boldsymbol{H}_t$ refer to the transverse (to x) electric and magnetic fields, respectively, and $\mathbf{x}_0$ is the unit vector in the x direction.

Fig. 1—Modulated plane reactive surface.

The waves guided by the surface are taken to propagate in the z direction, and, for simplicity, no variation is assumed present in either the geometry or the fields in the y direction. An E and H (or TM and TE) modal decomposition is always possible in the x direction for this geometry, but, because of the lack of dependence on y, these modes are identical with E and H modes viewed in the z direction. In the present paper, only the E mode solutions are considered because of their applicability to surface-wave antennas.

The total field is viewed in terms of modes defined with respect to propagation in the transverse, or x, direction. The corresponding vector mode functions $\boldsymbol{h}_n$ and $\boldsymbol{e}_n$, which form an orthonormal set, are[5]

$$\boldsymbol{h}_n(z) = \boldsymbol{e}_n(z) \times \mathbf{x}_0 = \mathbf{y}_0 \frac{1}{\sqrt{2\pi}} \exp\left[-j\left(\kappa + \frac{2n\pi}{a}\right)z\right], \tag{3}$$

where κ is the propagation wavenumber along the surface (in the z direction), and is related to the transverse wavenumber k_{tn} by

$$k_{tn} = \sqrt{k^2 - \left(\kappa + \frac{2n\pi}{a}\right)^2}, \qquad n = 0, \pm 1, \pm 2, \cdots, \tag{4}$$

k being the free-space wavenumber $(=2\pi/\lambda)$. With this notation, the total magnetic field, for example, is written

$$H_y(x, z) = \sum_{n=-\infty}^{\infty} I_n(x)h_n(z) \tag{5}$$

or

$$H_y(x, z) = e^{-j\kappa z} \sum_{n=-\infty}^{\infty} \frac{I_n(0)}{\sqrt{2\pi}} e^{-j(2n\pi/a)z} e^{-jk_{tn}x}, \tag{6}$$

which could alternatively have been obtained via Floquet's theorem. The transverse mode viewpoint is chosen here because it permits a clearer physical interpretation of the solution.

The mode voltage V_n of the nth transverse mode is

$$V_n(x) = \int_0^a \boldsymbol{E}_t(x, z) \cdot \boldsymbol{e}_n^*(z)dz, \tag{7}$$

which, in view of the boundary condition (2), becomes at $x=0$:

$$V_n(0) = j\int_0^a \left[1 + M\cos\frac{2\pi}{a}z\right] X_s H_y(0, z) e_n^*(z)dz. \tag{8}$$

When the mode function e_n from (3) is inserted into (8), and the relation for the transverse mode current I_n is recognized to be

$$I_n(x) = \int_0^a \boldsymbol{H}_t(x, z) \cdot \boldsymbol{h}_n^*(z)dz, \tag{9}$$

expression (8) becomes

$$V_n = jX_s I_n + jX_s \frac{M}{2}(I_{n+1} + I_{n-1}). \tag{10}$$

[5] N. Marcuvitz, "Waveguide Handbook," Rad. Lab. Series, McGraw-Hill Book Co., Inc., New York, N. Y., vol. 10, pp. 88, 89; 1951.

Relation (10) indicates that the nature of the boundary condition at $x=0$ is such that it couples each transverse mode to its nearest neighbors, rather than to all of the other transverse modes as usually occurs with diffracting surfaces.

The determinantal equation for the propagation characteristics of the guided waves, whether of modal or nonmodal (leaky wave) nature, may be phrased as the condition for resonance in the transverse plane. This transverse resonance condition states that at any cross-section (to x) plane, the sum of the impedances looking in both directions away from this plane must equal zero. At the $x=0$ plane, the impedance for the nth transverse mode looking toward the plane is obtainable from (10), while that looking outward is simply

$$\frac{V_n}{I_n} = Z_n = \frac{k_{tn}}{\omega\epsilon}. \tag{11}$$

Combining (11) with (10), one finds for the transverse resonance condition

$$I_{n+1} + D_n I_n + I_{n-1} = 0, \qquad n = 0, \pm 1, \pm 2, \cdots, \tag{12}$$

where

$$D_n = \frac{2}{M}\left[1 - j\frac{k_{tn}}{X_s\omega\epsilon}\right]. \tag{13}$$

The recurrence relation (12) may be viewed as an infinite set of linear homogeneous equations for the infinite number of unknown modal currents I_n. This set of equations possesses a nontrivial solution if the infinite determinant of the set vanishes. This condition may be rephrased in the following manner. Consider the semi-infinite set of these equations which begins at any finite value of n and contains those equations with lower values of n. From the first two equations of this set, one can write

$$\frac{I_n}{I_{n+1}} = -\cfrac{1}{D_n - \cfrac{1}{D_{n-1} + \cfrac{I_{n-2}}{I_{n-1}}}}.$$

Continuing in this fashion for the remainder of the semi-infinite set, one finds the continued fraction solution

$$\frac{I_n}{I_{n+1}} = -\cfrac{1}{D_n} - \cfrac{1}{D_{n-1}} - \cfrac{1}{D_{n-2}} - \cdots. \tag{14}$$

From the remaining semi-infinite set of equations one has, analogously,

$$\frac{I_{n+1}}{I_n} = -\cfrac{1}{D_{n+1}} - \cfrac{1}{D_{n+2}} - \cfrac{1}{D_{n+3}} - \cdots. \tag{15}$$

It can be shown[6] that if $|D_n| > 2$ for $n > n_0$, the continued fractions (14) and (15) converge; from (13) we see that $|D_n| \sim n$ for large n due to the presence of k_{tn} in the numerator of D_n.

In order that the infinite set of equations (12) have a non-vanishing solution, (14) must equal the inverse of (15). Thus, employing (13) and (4), one obtains for an inductive surface the following completely equivalent equations, one for each $n(=0, \pm 1, \pm 2, \cdots)$:

$$\begin{aligned}
&1 - \frac{j}{X_s'}\sqrt{1 - \left[\frac{\kappa}{k} + \frac{2\pi n}{ka}\right]^2} \\
&= \frac{M^2}{4}\left\{\cfrac{1}{1 - \cfrac{j}{X_s'}\sqrt{1 - \left[\frac{\kappa}{k} + \frac{2\pi(n-1)}{ka}\right]^2}} - \right. \\
&\quad - \cfrac{M^2/4}{1 - \cfrac{j}{X_s'}\sqrt{1 - \left[\frac{\kappa}{k} + \frac{2\pi(n-2)}{ka}\right]^2}} - \cdots \\
&\quad + \cfrac{1}{1 - \cfrac{j}{X_s'}\sqrt{1 - \left[\frac{\kappa}{k} + \frac{2\pi(n+1)}{ka}\right]^2}} - \\
&\quad \left. - \cfrac{M^2/4}{1 - \cfrac{j}{X_s'}\sqrt{1 - \left[\frac{\kappa}{k} + \frac{2\pi(n+2)}{ka}\right]^2}} - \cdots \right\},
\end{aligned} \tag{16}$$

where $X_s' = X_s/\sqrt{\mu/\epsilon}$. Due to the presence of the additional factor of $M^2/4$ in each successive term, the continued fractions converge rapidly for all values of modulation. For calculational purposes, n is set equal to zero in (16), and the five terms shown are sufficient to yield the solution for the propagation wavenumber κ to a high degree of accuracy in almost all cases.

By means of (14) and (15), one may evaluate the amplitudes of each of the space harmonics relative to, say, I_0. Since the ratio I_n/I_0 behaves asymptotically for large n as $1/n!$, the total field clearly converges. Thus, the solution presented above permits the calculation of the complete field distribution and the propagation characteristics to any desired degree of accuracy.

III. Discussions of Results

The guided-wave solutions to (16) are of two types, the (modal) surface waves, for which κ is real, and the (nonmodal) leaky waves, for which κ is complex. When the modulation spacing a is small, the guided wave is a (trapped) surface wave; when this spacing exceeds a critical value, a leaky wave is created and radiation occurs. The propagation behavior for each of these two wave types is discussed below.

[6] J. Meixner and F. W. Schäfke, "Mathieusche Funktionen und Sphäroidfunktionen," Springer Verlag, Berlin, Germany, pp. 89–93; 1954.

A. The (Trapped) Surface-Wave Solutions

For the surface-wave solution, κ is real and greater than k, corresponding to a slow wave, and all of the constituent space harmonics are also slow waves, with a field distribution that decays transversely to the guiding surface. Alternatively, all constituent transversely-directed modes are below cutoff in the x direction, so that k_{tn} is imaginary for all n, and the total field is confined to the neighborhood of the $x=0$ surface.

It can be shown that the allowed regions for the surface-wave solutions in a band structure plot is a succession of triangular areas with the tips of the triangles ending at $ka=\pi$, as shown in Fig. 2. Within each of these allowed areas, there also exists at least one stop band, the width of which is a function of the modulation depth. Typical band structure curves, for the case $X_s'=1$, are presented in Fig. 3 for three values of modulation amplitude M. The stop bands are seen to occur about $\kappa a=\pi\pm 2n\pi$; within the stop bands, the values of κ are complex. As expected, the width of the stop band is seen to be greater for larger values of M.

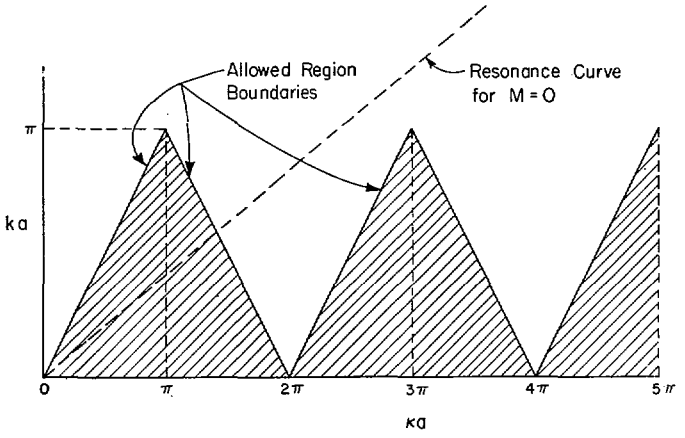

Fig. 2—Allowed regions for (trapped) surface-wave solutions.

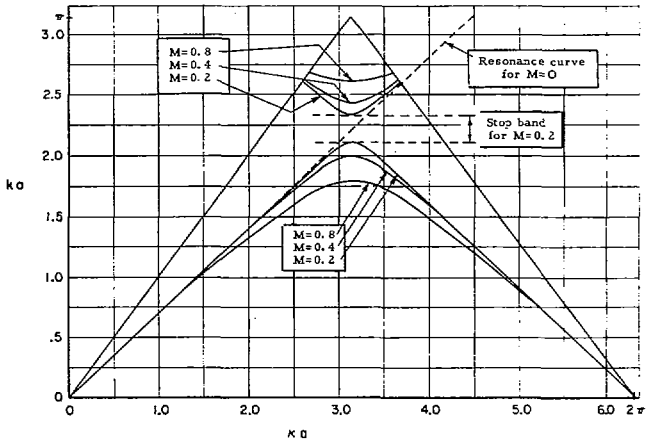

Fig. 3—Band structure curves for surface-wave solutions for various modulation depths, for $X_s'=1$.

The behavior at the band edges of the upper band is also of interest. Although not apparent in Fig. 2, due to the scale employed, the curves turn around at the band edges to become parallel to the allowed region boundaries.

The effect on the band structure curves of different average surface reactance values X_s', for fixed M, is indicated in Fig. 4. It is seen that the curves follow the straight resonance lines obtained for $M=0$ for the corresponding values of X_s'. The middle curve, for $X_s'=1$ and $M=0.4$, is a duplicate of the middle curve of Fig. 3. The curve for $X_s'=0.2$ corresponds to a very loosely-bound wave, and, consequently, to a wave with a phase velocity very close to that of the velocity of light. It is noted that for this case the stop band is very small and is located near to the tip of the allowed region. Of particular interest is the $X_s'=5$ case, which corresponds to a very tightly-bound wave. It is seen that *more than one* stop band is obtained for this case. (For clarity, the repetition of the curves from one triangle to another, required for a complete band structure presentation, has been omitted.) Thus, as ka increases, the wave type changes from a purely trapped surface wave to a leaky wave and then back to a surface wave again for a band of ka. Such behavior, with associated multiple stop bands, is obtained when $X_s'>\sqrt{8}$. It is easily shown that n stop bands are present if $(2n-1)^2-1<(X_s')^2<(2n+1)^2-1$. Thus, three stop bands are actually present for $X_s'=5$, but since the third stop band occurs very near to the tip of the third triangle, it has been ignored in Fig. 4.

The relative amplitudes of the space harmonics constituting the surface wave are indicated graphically in Fig. 5 for the case $X_s'=1$, $M=0.4$, as a function of ka for the lower band. It is seen that to a good approximation only the fundamental and a single space harmonic ($n=-1$) need be considered. It is also noted that at the onset of the stop band, the amplitudes of the first backward-traveling space harmonic and the forward-traveling fundamental are equal, *i.e.*, $I_{-1}/I_0=1$, and that the amplitudes of the remaining forward- and backward-traveling space harmonics also become equal in pairs so as to establish a standing wave. This behavior is typical of that occurring in stop bands of periodic structures, and affords a check on the analysis.

As an illustration of the space harmonic content of the surface wave as a function of average surface reactance X_s', the ratio I_-/I_0 is plotted as a function of κa in Fig. 6 for three different values of X_s', keeping M constant. It is seen that the amplitude of the $n=-1$ space harmonic increases as the wave becomes more tightly bound. The same behavior also results for the other space harmonics.

Since more than one stop band is found to exist for the case $X_s'=5$ (see Fig. 4), a plot of the relative amplitudes for this case serves to indicate the differences in

space harmonic content that occur in the upper and lower pass bands and in successive triangles. The relative amplitude curves for the first triangle are given in Fig. 7. It is seen that the curves for the lower pass band are similar in form to those appearing in Fig. 5 for a different value of X_s'. The curves in the upper band, however, have a different form from those in the lower band. The relative amplitudes for the second triangle (see the corresponding band structure curve in Fig. 4) are presented in in Fig. 8. It is noted that the space harmonic content is quite different in the second triangle, and that more space harmonics are required to properly characterize the field.

Since a standing wave is established at the band edges of the stop band, certain necessary relations between the amplitudes must exist. It can readily be shown that these relations are: For the first triangle:

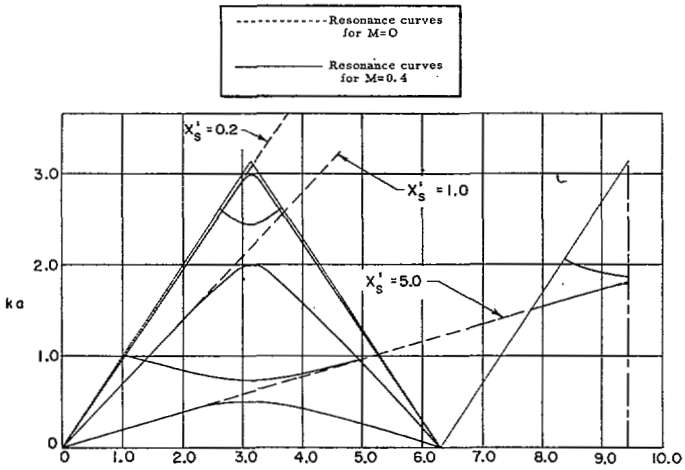

Fig. 4—Band structure curves for surface-wave solutions for various average surface reactances, for $M=0.4$.

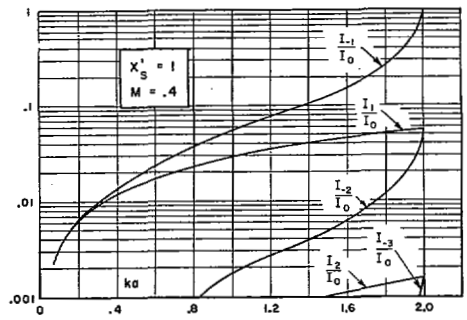

Fig. 5—Relative amplitudes of the space harmonics of the surface wave in the lower band.

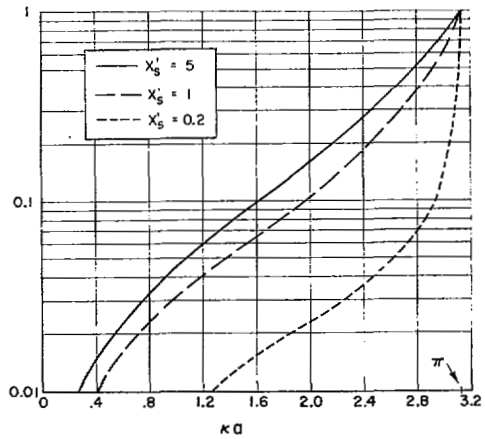

Fig. 6—Relative amplitudes of the $n=-1$ space harmonic for various surface reactances, for $M=0.4$.

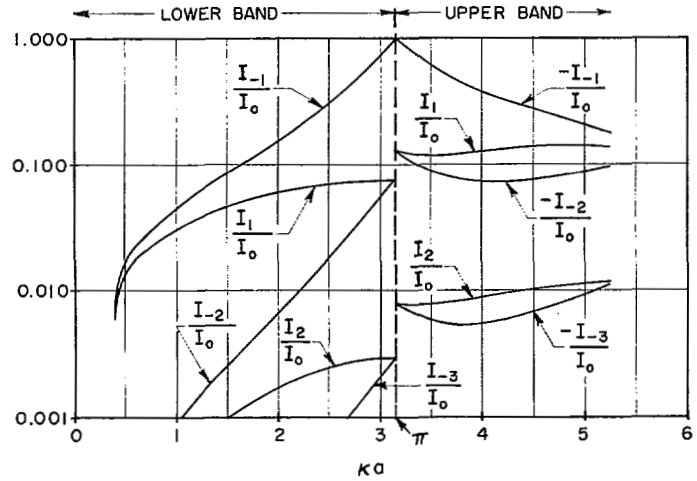

Fig. 7—Relative amplitudes of the space harmonics of the surface waves in the upper and lower bands in the first triangle for $X_s'=5$, $M=0.4$.

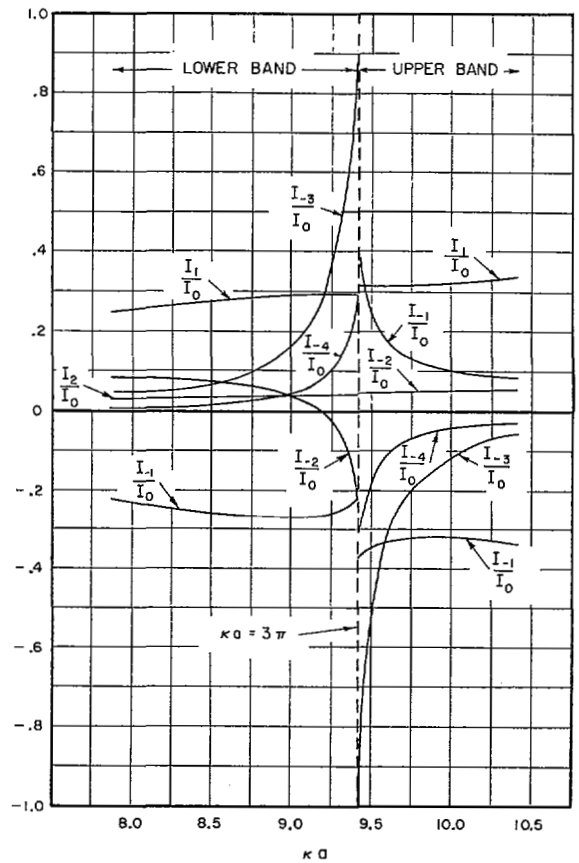

Fig. 8—Relative amplitudes of the space harmonics of the surface waves in the second triangle for $X_s'=5$, $M=0.4$.

$$I_{-1} = \pm I_0, \quad I_{-2} = \pm I_1, \cdots I_{-n} = \pm I_{n-1}.$$

For the second triangle:

$$I_{-3} = \pm I_0, \quad I_{-2} = \pm I_{-1}, \cdots I_{-n} = \pm I_{n-3}.$$

The upper and lower signs refer to the lower and upper bands, respectively. The involved behavior of the curves in Fig. 8 is readily explainable in terms of these relations.

B. The Leaky Wave Solutions

When ka is raised sufficiently so that a surface wave solution is no longer possible, the $n=-1$ transversely-directed mode is raised above cutoff, corresponding to a *propagating* wave in the direction perpendicular to the surface, while the remainder of these modes are still substantially below cutoff in this direction. As a result, the value of κ from (16) becomes complex. As the value of ka is raised further, additional transversely-directed modes may become propagating. Each of these modes remains above cutoff for only a limited range of ka, however, so that only a small number of these modes may be propagating for any value of ka. This number is a function of the average surface reactance X_s.

If β_u represents the unperturbed value of κ, corresponding to $M=0$, the value of κ in the leaky wave region may be written as

$$\kappa = \beta_u + \Delta\beta - j\alpha. \tag{17}$$

When the transverse wavenumbers k_{tn} are examined consistent with form (17) for κ, one finds that those transversely-directed modes which are *above* cutoff correspond to *outgoing* waves in the transverse direction, with an exponential amplitude increase in this direction if the wave is directed forward and a decrease if it is directed backward. All of the other transversely-directed modes exhibit the exponential transverse decay associated with their cutoff nature, but possess a small phase variation corresponding to an incoming wave for the forward-traveling space harmonics and to an outgoing wave for the backward-traveling space harmonics.

Those space harmonics corresponding to $n \geq 0$ are always forward-traveling waves and always remain essentially below cutoff. A given space harmonic for which n is negative is a backward-traveling wave which is below cutoff (in the surface wave region) or essentially below cutoff (in the leaky wave region) for the smaller values of ka. If ka is raised sufficiently, the wave changes into an essentially propagating wave which first propagates in the *backward* direction. As ka is increased further, the radiating wave swings up, passes through broadside and approaches the forward end-fire position. As ka is raised still further, the wave becomes essentially below cutoff again and, for all higher ka values, remains a *forward-traveling* space harmonic.

It is convenient to employ a perturbation solution of (16) for the rapid evaluation of the complex κ value for small values of modulation. The perturbation is taken about the $M=0$ value to yield

$$\Delta\beta a - j\alpha a = -\frac{M^2}{4}\frac{kaX_s'^2}{\sqrt{1+X_s'^2}} \cdot \left[\frac{1}{1-\frac{j}{X_s'}\sqrt{1-\left[\sqrt{1+X_s'^2}-\frac{2\pi}{ka}\right]^2}} + \frac{1}{1-\frac{j}{X_s'}\sqrt{1-\left[\sqrt{1+X_s'^2}+\frac{2\pi}{ka}\right]^2}}\right]. \tag{18}$$

Expression (18) takes into account only the $n=0$, 1, and -1 transversely-directed modes (or space harmonics), and yields accurate results except within certain narrow ranges of ka.

A plot of the attenuation constant as a function of ka is presented in Fig. 9 for the case $X_s'=1$, $M=0.4$. To this order, the behavior is strongly associated with that for the $n=-1$ transversely-directed mode. Perturbation formula (18) is inadequate when the radiating beam corresponding to the $n=-1$ term points in the broadside direction, or in either the forward or backward end-fire directions. In these "transition" regions more space harmonics are required to describe the behavior accurately. For this reason, the curve of Fig. 9 avoids both end-fire regions; it should also be understood, however, that the curve is incorrect in the vicinity of broadside radiation, *i.e.*, around $ka=4.4$.

The modulation also serves to alter the guide wavelength slightly, and the change $\Delta\beta$ in the phase constant computed via relation (18) is plotted in Fig. 10 as a function of ka. It is seen that the change is such as to decrease β for the smaller ka values, but to increase it

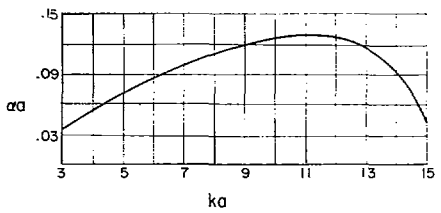

Fig. 9—Attenuation constant of leaky wave as a function of ka, computed to first order, for $X_s'=1$, $M=0.4$.

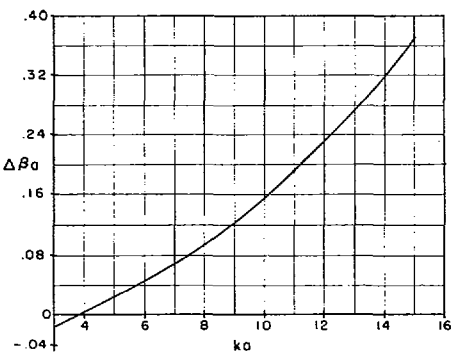

Fig. 10—Change in phase constant of leaky wave as a function of ka, computed to first order, for $X_s'=1$, $M=0.4$.

as ka is increased. The remarks regarding the inadequacy of (18) for the attenuation constant apply also to $\Delta\beta$.

The amplitude ratios of the space harmonics, or alternatively, of the transversely-directed modal constituents of the leaky wave, are now complex, but to first order, consistent with perturbation result (18), only those ratios involving radiating beams are complex. It is found that for all but certain narrow ranges of ka (corresponding to the above-mentioned "transition" regions), for which the amplitude of a particular space harmonic may become large, all field amplitudes are small except for I_0, I_{-1} and I_1, with I_0 dominant.

The magnitudes and phases of the relative amplitudes in the leaky wave region for the case $X_s'=1$, $M=0.4$ are presented in Figs. 11 and 12. With regard to the magnitudes plotted in Fig. 11, it is seen that only $n=1$ and $n=-1$ terms are significant relative to the fundamental ($n=0$) over the whole range of ka covered in the figure. The ratio $|I_{-2}/I_0|$ remains small except in the vicinity of $ka=4.4$, which is a "transition" region corresponding to broadside radiation for the $n=-1$ beam. To first order, this ratio becomes infinite; when more space harmonics are taken into account, the resulting more accurate calculation yields a finite maximum value. From Fig. 12, one notes that the ratios I_1/I_0 and I_2/I_0 are real. A π phase shift in I_{-2}/I_0 is seen to occur at the value of ka corresponding to the peak in the magnitude of this ratio. Except for this jump, the values of phase are seen to be constant or slowly-varying.

A few brief remarks are made below on the application of these studies to the antenna problem. As mentioned above, the first radiating beam that appears as ka is raised is at first directed backwards, along the surface in the negative z direction, as is well-known from array considerations. As ka is raised further, this beam swings up through broadside and eventually reaches the forward end-fire position before vanishing. However, unless λ/λ_g is greater than three (corresponding to $X_s'>\sqrt{8}$), at least one additional beam will be present, directed at some angle, while the original beam is in the forward end-fire position. (If no additional beam is present, more than one stop band will occur and the appropriate band structure curves are similar to those shown in Fig. 4 for $X_s'=5$.) The case for which two beams are present is illustrated in Fig. 13.

It is clear that, by proper choice of the average surface reactance value X_s', one can eliminate the presence of unwanted additional beams. However, this requires a very tightly-bound surface wave, with attendant higher space-harmonic content. It is customary to employ a less tightly-bound wave, with the result that one or

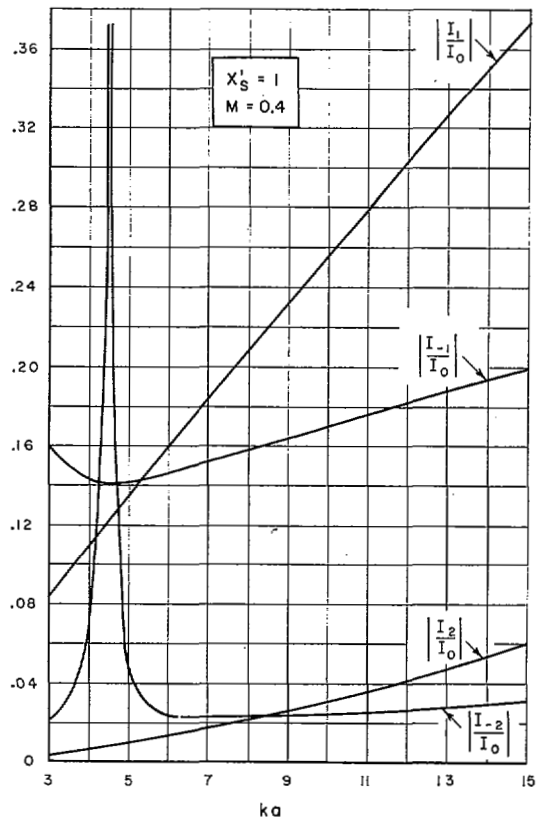

Fig. 11—Magnitude of the complex amplitudes of the space harmonics of the leaky wave as a function of ka, computed to first order, for $X_s'=1$, $M=0.4$.

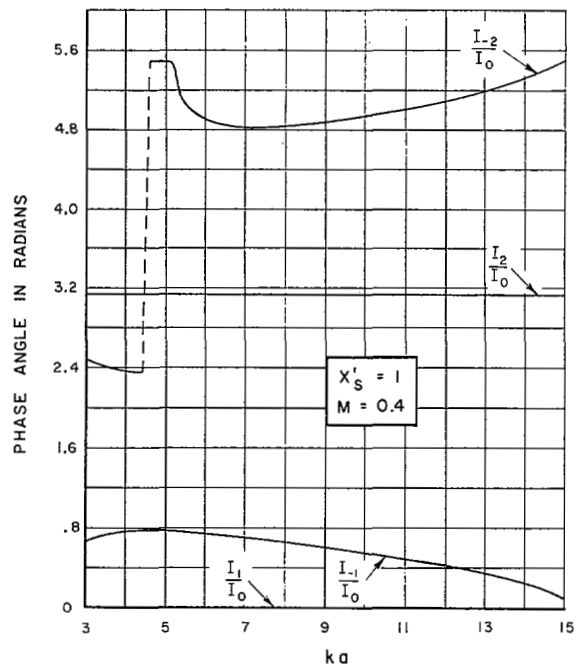

Fig. 12—Phase of the complex amplitudes of the space harmonics of the leaky wave as a function of ka, computed to first order, for $X_s'=1$, $M=0.4$.

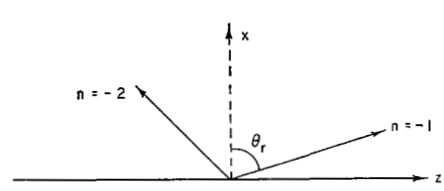

Fig. 13—Illustration of two radiating beams in the leaky wave region. Angle θ_r is the real part of complex angle θ, defined by $\cos\theta=k_t/k$.

more additional beams may be present. If a significant amount of power is carried by any of these additional beams, their influence on the desired radiation pattern will not be negligible. While in the presence of radiation loss power orthogonality no longer exists rigorously between the individual transversely-directed modes, the square of the amplitude ratios is nevertheless a reasonably good measure of the power radiated if the attenuation constant remains small.

The antenna design may require the radiated beam to appear at any desired angle, say at $\theta_r = 30°$ in Fig. 13. For such an angle, away from the "transition" regions, the perturbation results are accurate. For the case $X_s' = 1$, $M = 0.4$, this angle corresponds to $ka \approx 6.9$, and one additional beam is present, at the angle $\theta_r \approx -25°$. The ratio $|I_{-2}/I_{-1}|$ at this value of ka is approximately 0.14, so that the power radiated by the additional beam is only about 2 per cent of that radiated by the desired beam. Since this ratio is proportional, to first order, to the modulation depth M, the ratio of radiated powers would be reduced by a factor of about four if M had been chosen to be 0.2, rather than 0.4. The attenuation constant α thus represents essentially the leakage into the desired beam only. The radiation pattern may then be determined by standard techniques; if the antenna is long and the leakage is slow, a very narrow beam can be obtained.

The motivation for this study was related to forward end-fire radiation, *i.e.*, $\theta_r = 90°$ in Fig. 13. The same considerations discussed above for $\theta_r = 30°$ apply to the end-fire case, except for the validity of the perturbation expression (18), which affects only the detailed numerical values. Thus, the high-gain end-fire antenna of the modulated surface wave type is in reality a form of *leaky wave* antenna. With a long structure designed for slow leakage, a high end-fire gain is seen to be achievable.

ACKNOWLEDGMENT

The authors wish to thank F. J. Zucker of the Air Force Cambridge Research Center for many stimulating discussions on the subject of modulated surface-wave antennas.